Model Order Reduction of Parameterized Interconnect Networks via a Two-Directional Arnoldi Process

Yung-Ta Li, Zhaojun Bai, Yangfeng Su, and Xuan Zeng, *Member, IEEE*

***Abstract*—This paper presents a multiparameter moment-matching-based model order reduction technique for parameterized interconnect networks via a novel two-directional Arnoldi process (TAP). It is referred to as a Parameterized Interconnect Macromodeling via a TAP (PIMTAP) algorithm. PIMTAP inherits the advantages of previous multiparameter moment-matching algorithms and avoids their shortfalls. It is numerically stable and adaptive. PIMTAP model yields the same form of the original state equations and preserves the passivity of parameterized RLC networks like the well-known method passive reduced-order interconnect macromodeling algorithm for nonparameterized RLC networks.**

***Index Terms*—Arnoldi process, moment matching, parameterized model order reduction (PMOR).**

I. Introduction

With THE decrease of IC feature size and the increase of signal frequency, interconnect has become a dominant factor for the determination of the whole chip performance. Interconnect networks are typically represented by large-scale system equations with respect to frequency parameter. However, during the circuit synthesis of large-scale digital or analog applications, it is also crucial to evaluate the response of interconnect as functions of other design parameters, such as geometry and temperature. In these cases, parameterized model order reduction (PMOR) methods are necessary simulation techniques for the analysis of parameterized interconnect circuits. In addition, the indetermination in the manufacturing of IC chips also causes system variations of critical dimensions and interlevel dielectric thicknesses of interconnects, which could make the chip performance unpredictable and cause significant parametric yield lose. Therefore, it becomes necessary to use PMOR methods for the analysis of interconnect system in the presence of process variations [1]–[8].

A number of PMOR methods have been developed for modeling large-scale parameterized interconnect systems. The perturbation technique [5] is one of the early work to capture small variation around the nominal circuit values. It becomes inefficient when modeling strong nonlinear effects caused by the intradie variations [7]. Multiparameter moment-matching methods [3], [9] preserve the structure and, therefore, guarantee the passivity. However, the computational procedures of the methods are potentially numerical unstable due to the fact that the basis vectors of the underlying projection subspace are explicitly calculated. To overcome the numerical instability, in [10] and [11], it is proposed to first find a linear combination of the basis vectors with respect to an orthonormal basis and performs matrix-vector products on the orthonormal basis. However, it is not a fully implicit method and could still be numerically unstable. In [12], the projection subspace for moment matching is defined as a union of Krylov subspaces. As a result, the number of Krylov basis vectors needed to be computed is substantially larger than the dimensionality of the required projection subspace. The method proposed in [13] and [14] uses a multiseries expansion of the transfer function to generate the projection matrix. However, the method is difficult to generalize to several parameters. The Compact Order Reduction for parameterized Extraction (CORE) algorithm [7] is an explicit-and-implicit scheme. Unfortunately, it does not preserve the structure of the state equation form and, therefore, does not preserve the passivity.

Truncated balance realization-based approaches have also been extended for variational MOR [8], [15]. In general, the approaches have high computational complexity due to a large amount of sampling points typically required to calculate the system Grammians. Stochastic spectral Galerkin method is another approach for analyzing interconnect circuits [1] and power grid circuits [16] with process variations. Homogeneous chaos is applied in the approach to capture the impact of process variations on the interconnect response. However, this method cannot be regarded as a true PMOR method, and it does not preserve the structure of the state equations. Rational interpolation-based methods are proposed for including

Manuscript received August 23, 2007; revised January 31, 2008. Published August 20, 2008 (projected). The work of Y.-T. Li and Z. Bai was supported in part by the National Science Foundation under Grant DMS-0611548. The work of Y. Su was supported in part by Shanghai Dawn Project 200601 and in part by China NSF Project 90307017. The work of X. Zeng was supported in part by China NSF Projects 90307017 and 60676018, in part by the National Basic Research Program of China under Grant 2005CB321701, and in part by the Doctoral Program Foundation of the Ministry of Education of China (20050246082). This paper was recommended by Associate Editor R. Suaya.

Y.-T. Li is with the Department of Mathematics, University of California, Davis, CA 95616 USA (e-mail: ytli@math.ucdavis.edu).

Z. Bai is with the Department of Computer Science and Department of Mathematics, University of California, Davis, CA 95616 USA (e-mail: bai@cs.ucdavis.edu).

Y. Su is with the School of Mathematical Sciences, Fudan University, Shanghai 200433, China (e-mail: yfsu@fudan.edu.cn).

X. Zeng is with the State Key Laboratory of Application Specific Integrated Circuits and Systems, Microelectronics Department, Fudan University, Shanghai 200433, China (e-mail: xzeng@fudan.edu.cn).

Color versions of one or more of the figures in this paper are available online at http://ieeexplore.ieee.org.

Digital Object Identifier 10.1109/TCAD.2008.927768

variations of electrical and geometrical parameters in macromodels of lossy transmission lines [17] and for RF inductor design [18]. These methods have been applied for frequency domain identification.

In this paper, we present a multiparameter moment-matching-based PMOR technique for parameterized RLC interconnect networks via a novel two-directional Arnoldi process (TAP). We call it the Parameterized Interconnect Macromodeling via a TAP (PIMTAP) algorithm. The PIMTAP algorithm inherits the advantages of multiparameter moment-matching-based methods, such as multivariable Taylor series approach [9] and the CORE algorithm [7]. However, it avoids their shortfalls. PIMTAP method is computationally stable and robust. PIMTAP model preserves the structure of the original state equations like passive reduced-order interconnect macromodeling algorithm [19] for nonparameterized RLC networks.

All multiparameter moment-matching-based PMOR techniques, including the one proposed in this paper, are designed for a low-dimensional parameter space. Variations in modern VLSI technologies sometimes introduce a high-dimensional parameter space. It is referred to as the *curse of dimensionality*. In [20], a two-step approach is introduced to construct a compact model of parameterized system. The first step is for parameter reduction to reduce high-dimensional parameter space. The second step is to construct a reduced-order model by applying a PMOR technique. Moment-matching techniques discussed in this paper are intended for the application of the second step.

The remainder of this paper is organized as follows. In Section II, we review the system equations, the series expansion of the transfer function, and the MOR framework via subspace projection. Section III reviews related multiparameter moment-matching methods presented in [7], [9], [13], and [14]. In Section IV, we present the PIMTAP algorithm for systems of single geometric parameter. The extension of the PIMTAP algorithm to multiple geometric parameter systems is described in Section V. Numerical results, including the comparison with the CORE method, are presented in Section VI. Concluding remarks are presented in Section VII.

II. Background

We consider a single-input and single-output parameterized linear dynamical system of the form

$$\begin{cases} \mathbf{C}(\lambda)\dot{\mathbf{x}} + \mathbf{G}(\lambda)\mathbf{x} = \mathbf{b}u \\ y = \mathbf{l}^{\mathrm{T}}\mathbf{x} \end{cases} \tag{1}$$

with initial conditions $\mathbf{x}(\lambda, 0) = \mathbf{x}_0(\lambda)$, where $\lambda = (\lambda_1, \lambda_2, \ldots, \lambda_k)$ are parameters. The matrices $\mathbf{C}(\lambda)$ and $\mathbf{G}(\lambda)$ are of *affine* forms

$$\begin{aligned} \mathbf{C}(\lambda) &= \mathbf{C}_0 + \lambda_1\mathbf{C}_1 + \cdots + \lambda_k\mathbf{C}_k, \\ \mathbf{G}(\lambda) &= \mathbf{G}_0 + \lambda_1\mathbf{G}_1 + \cdots + \lambda_k\mathbf{G}_k \end{aligned} \tag{2}$$

where $\mathbf{C}_i$ and $\mathbf{G}_i$ are $N \times N$ constant matrices. $\mathbf{b}$ is an excitation vector, and $\mathbf{l}$ is a selector vector of the output of interest y. $\mathbf{x}$ is a state vector of the system.

The linear dynamical system (1) of the affine form (2) arises from parameterized interconnect networks, where $\mathbf{C}(\lambda)$ and $\mathbf{G}(\lambda)$ are the contributions of parameter dependent memory and memoryless elements of the network [5], [9], [21], [22]. The parameters λ_i represent the geometry of the network, such as the width and height of an interconnect line and are referred to as *geometric* parameters in [9]. In [12] and [23], the finite element analysis of parametric electrothermal simulation of a microelectromechanical system (MEMS) also gives rise to the affine model (2). Linear systems of the polynomial form have also been considered [7], [10], [11]. More general forms of system matrices $\mathbf{G}(\lambda)$ and $\mathbf{C}(\lambda)$ could be approximated through power series expansion and truncation [7], [22]. PIMTAP method discussed in this paper can be extended to treat the polynomial form and will be presented elsewhere.

In this section, for the clarity of exposition, we only consider the affine system of a single parameter

$$\begin{cases} (\mathbf{C}_0 + \lambda\mathbf{C}_1)\dot{\mathbf{x}} + (\mathbf{G}_0 + \lambda\mathbf{G}_1)\mathbf{x} = \mathbf{b}u \\ y = \mathbf{l}^{\mathrm{T}}\mathbf{x} \end{cases} \tag{3}$$

and λ is a scalar. Through this paper, it is assumed that $\mathbf{G}_0$ is nonsingular. In Section V, we will discuss multiparameter systems that is $k \geq 2$ in (2).

By the Laplace transform, the behavior of the system (3) in frequency domain is characterized by the *transfer function*

$$h(s, \lambda) = \mathbf{l}^{\mathrm{T}} \left(\mathbf{G}_0 + \lambda\mathbf{G}_1 + s(\mathbf{C}_0 + \lambda\mathbf{C}_1)\right)^{-1} \mathbf{b} \tag{4}$$

$$= \left(\sum_{i=0}^{\infty} m_i^j s^i\right) \lambda^j \tag{5}$$

where $s = 2\pi f\mathtt{i}$, f is referred to as the *frequency* and $\mathtt{i} = \sqrt{-1}$. $m_i^j = \mathbf{l}^{\mathrm{T}}\mathbf{r}_i^j$ are referred to as *(multiparameter) moments*. The vectors $\mathbf{r}_i^j$ are *moment generating vectors* defined by the following two-directional recurrence:

$$\mathbf{r}_i^j = -\mathbf{G}_0^{-1}\left(\mathbf{C}_0\mathbf{r}_{i-1}^j + \mathbf{G}_1\,\mathbf{r}_i^{j-1} + \mathbf{C}_1\,\mathbf{r}_{i-1}^{j-1}\right) \tag{6}$$

with $\mathbf{r}_0^0 = \mathbf{G}_0^{-1}\mathbf{b}$ and $\mathbf{r}_i^j = \mathbf{0}$ if $i < 0$ or $j < 0$.

We pursue a moment-matching-based algorithm by a subspace projection technique presented in [4], [19], [24]. Specifically, let $\mathbf{V}$ be an orthonormal basis of a proper defined projection subspace $\mathcal{V}$ of dimension n, $n \leq N$, and let the state variable

$$\mathbf{x} \approx \mathbf{V}\mathbf{z}$$

where $\mathbf{z}$ is a vector of dimension n. Substituting $\mathbf{x}$ by $\mathbf{V}\mathbf{z}$ into (3) and premultiplying the equation (3) by $\mathbf{V}^{\mathrm{T}}$, we derive the following reduced-order model:

$$\begin{cases} (\widehat{\mathbf{C}}_0 + \lambda\widehat{\mathbf{C}}_1)\dot{\mathbf{z}} + (\widehat{\mathbf{G}}_0 + \lambda\widehat{\mathbf{G}}_1)\mathbf{z} = \widehat{\mathbf{b}}u \\ \widehat{y} = \widehat{\mathbf{l}}^{\mathrm{T}}\mathbf{z} \end{cases} \tag{7}$$

where $(\widehat{\mathbf{C}}_0, \widehat{\mathbf{C}}_1, \widehat{\mathbf{G}}_0, \widehat{\mathbf{G}}_1) \equiv \mathbf{V}^{\mathrm{T}}(\mathbf{C}_0, \mathbf{C}_1, \mathbf{G}_0, \mathbf{G}_1)\mathbf{V}$ and $(\widehat{\mathbf{b}}, \widehat{\mathbf{l}}) \equiv \mathbf{V}^{\mathrm{T}}(\mathbf{b}, \mathbf{l})$. Similar to (4) and (5), the transfer function

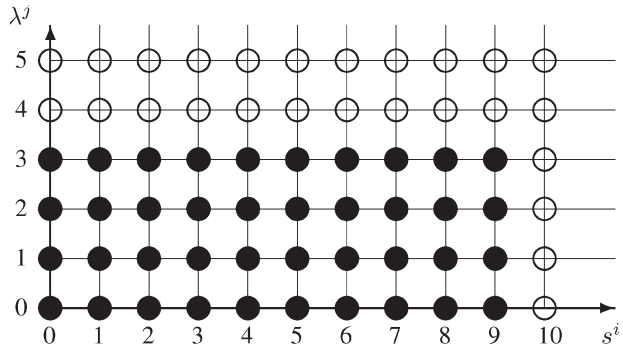

Fig. 1. Forty matched moments are the filled circles when $(p, q) = (9, 3)$.

of the reduced-order system (7) is given by

$$\begin{aligned}\widehat{h}(s,\lambda) &= \widehat{\mathbf{l}}^{\mathrm{T}}\left(\widehat{\mathbf{G}}_0 + \lambda\widehat{\mathbf{G}}_1 + s(\widehat{\mathbf{C}}_0 + \lambda\widehat{\mathbf{C}}_1)\right)^{-1}\widehat{\mathbf{b}} \\ &= \sum_{j=0}^{\infty}\left(\sum_{i=0}^{\infty}\widehat{m}_i^j s^i\right)\lambda^j\end{aligned}$$

where $\widehat{m}_i^j = \widehat{\mathbf{l}}^{\mathrm{T}}\widehat{\mathbf{r}}_i^j$ are (multiparameter) moments and the moment generating vectors $\widehat{\mathbf{r}}_i^j$ satisfy the recurrence relation

$$\widehat{\mathbf{r}}_i^j = -\widehat{\mathbf{G}}_0^{-1}\left(\widehat{\mathbf{C}}_0\widehat{\mathbf{r}}_{i-1}^j + \widehat{\mathbf{G}}_1\widehat{\mathbf{r}}_i^{j-1} + \widehat{\mathbf{C}}_1\widehat{\mathbf{r}}_{i-1}^{j-1}\right) \tag{8}$$

with $\widehat{\mathbf{r}}_0^0 = \widehat{\mathbf{G}}_0^{-1}\widehat{\mathbf{b}}$, and $\widehat{\mathbf{r}}_i^j = \mathbf{0}$ if $i < 0$ or $j < 0$.

Given desired approximation orders p and q of frequency parameter s and geometric parameter λ, respectively, our goal is to define a proper projection subspace $\mathcal{V}$ such that the reduced-order system matches the following $(p+1)(q+1)$ moments:

$$m_i^j = \widehat{m}_i^j, \qquad i = 0:p, j = 0:q. \tag{9}$$

This implies that the reduced transfer function $\widehat{h}(s,\lambda)$ is an order-(p,q) approximation of $h(s,\lambda)$

$$\begin{aligned}h(s,\lambda) - \widehat{h}(s,\lambda) = &\underbrace{\sum_{i=p+1}^{\infty}\left(\sum_{j=0}^{q}\left(m_i^j - \widehat{m}_i^j\right)\lambda^j\right)s^i}_{\mathcal{O}(s^{p+1})} \\ &+ \underbrace{\sum_{j=q+1}^{\infty}\left(\sum_{i=0}^{\infty}\left(m_i^j - \widehat{m}_i^j\right)s^i\right)\lambda^j}_{\mathcal{O}(\lambda^{q+1})}.\end{aligned}$$

Fig. 1 shows that the total of 40 moments matched by $\widehat{h}(s,\lambda)$ when $(p,q) = (9,3)$. Therefore, the gists of a moment-matching PMOR method are the choice of the projection subspace $\mathcal{V}$ and a stable and efficient algorithm to generate an orthonormal basis $\mathbf{V}$ of $\mathcal{V}$.

III. Previous Work

A multivariable Taylor series method is proposed in [9]. By introducing an auxiliary parameter $\mu = s\lambda$ and using the multivariable Taylor series expansion, the transfer function (4) can be written as

$$h(\lambda, s, \mu) = \sum_{k=0}^{\infty}\sum_{j=0}^{k}\sum_{i=0}^{k-j} m_{i,j,k}\lambda^{k-(i+j)}s^i\mu^j$$

where $m_{i,j,k} = \mathbf{l}^{\mathrm{T}}\mathbf{f}_{i,j,k}$ are the *multiparameter moments*, and

$$\mathbf{f}_{i,j,k} = -\mathbf{G}_0^{-1}(\mathbf{C}_0\mathbf{f}_{i-1,j,k-1} + \mathbf{G}_1\mathbf{f}_{i,j,k-1} + \mathbf{C}_1\mathbf{f}_{i,j-1,k-1}) \tag{10}$$

with the initial $\mathbf{f}_{0,0,0} = \mathbf{G}_0^{-1}\mathbf{b}$, where $\mathbf{f}_{i,j,k} = \mathbf{0}$, if $i, j, i+j \notin \{0, 1, \ldots, k\}$. To match the $(p+1)(q+1)$ moments defined in (9), the dimension of the projection subspace span$\{\mathbf{f}_{i,j,k}\}$ has to be $\mathcal{O}((p+q)^3)$.

A multiseries expansion method proposed in [13] and [14] uses a different approach to expand the transfer function into a series. Under the assumption of the coefficient matrix $\mathbf{C}_1 = \mathbf{0}$, a series expansion of the transfer function $h(s,\lambda)$ is

$$h(s,\lambda) = \mathbf{l}^{\mathrm{T}}\left(\sum_{i=0}^{\infty}\mathbf{r}^{(i)}(s)\lambda^i\right).$$

Here, $\mathbf{r}^{(i)}(s)$ is defined and expanded into a series of s as follows:

$$\begin{aligned}\mathbf{r}^{(i)}(s) &= \left[-(\mathbf{G}_0 + s\mathbf{C}_0)^{-1}\mathbf{G}_1\right]^i(\mathbf{G}_0 + s\mathbf{C}_0)^{-1}\mathbf{b} \\ &= \sum_{\ell_i=0}^{\infty}\cdots\sum_{\ell_1=0}^{\infty}\sum_{\ell_0=0}^{\infty}\mathbf{r}_{\ell_i,\ldots,\ell_1,\ell_0}s^{\ell_i}\ldots s^{\ell_1}s^{\ell_0}\end{aligned}$$

where

$$\begin{aligned}\mathbf{r}_{\ell_i,\ldots,\ell_1,\ell_0} = (-1)^i&\left(\prod_{k=1}^{i}\left(-\mathbf{G}_0^{-1}\mathbf{C}_0\right)^{\ell_k}\left(-\mathbf{G}_0^{-1}\mathbf{G}_1\right)\right) \\ &\times\left(-\mathbf{G}_0^{-1}\mathbf{C}_0\right)^{\ell_0}\left(\mathbf{G}_0^{-1}\mathbf{b}\right).\end{aligned}$$

To match the $(p+1)(q+1)$ moments defined in (9), the dimension of the projection subspace span$\{\mathbf{r}_{\ell_i,\ldots,\ell_1,\ell_0}\}$ has to be $\mathcal{O}((p+1)^{q+1})$.

An explicit-and-implicit moment-matching technique, referred to as CORE algorithm, is proposed [7]. It has two steps. First, it defines the following linear system to *explicitly* approximate the geometric parameter λ to the qth order:

$$\begin{cases}(\mathbf{G}_{[q+1]} + s\mathbf{C}_{[q+1]})\widetilde{\mathbf{x}}_{[q+1]} = \widetilde{\mathbf{b}}_{[q+1]}\tilde{u} \\ \tilde{y}_{[q+1]} = \left(\mathbf{l}_{[q+1]}(\lambda)\right)^{\mathrm{T}}\tilde{\mathbf{x}}_{[q+1]}\end{cases} \tag{11}$$

where $\mathbf{G}_{[q+1]}$ and $\mathbf{C}_{[q+1]}$ are $(q+1)$ by $(q+1)$ block lower bidiagonal matrices and $\widetilde{\mathbf{b}}_{[q+1]}$ and $\mathbf{l}_{[q+1]}(\lambda)$ are column vectors. It is easy to see that the transfer function of (11) is an order-q approximation of the transfer function of the original system (3) in λ. At the second step, CORE applies the subspace projection method with the Krylov subspace

$$\mathcal{V} = \mathcal{K}_{p+1}\left(-\mathbf{G}_{[q+1]}^{-1}\mathbf{C}_{[q+1]}, \mathbf{G}_{[q+1]}^{-1}\widetilde{\mathbf{b}}_{[q+1]}\right)$$

to *implicitly* match the moments of s. A so-called *recursive Arnoldi algorithm* is used to generate an orthonormal basis $\mathbf{V}$ of $\mathcal{V}$, which effectively utilizes the block lower triangular structures of $\mathbf{G}_{[q+1]}$ and $\mathbf{C}_{[q+1]}$. The reduced-order model is then defined by

$$\begin{cases} (\widehat{\mathbf{G}}_{[q+1]} + s\widehat{\mathbf{C}}_{[q+1]})\tilde{\mathbf{z}}_{[q+1]} = \widehat{\mathbf{b}}_{[q+1]}\tilde{u} \\ \widehat{\tilde{y}}_{[q+1]} = \left(\widehat{\mathbf{l}}_{[q+1]}(\lambda)\right)^{\mathrm{T}} \tilde{\mathbf{z}}_{[q+1]} \end{cases} \tag{12}$$

where $(\widehat{\mathbf{G}}_{[q+1]}, \widehat{\mathbf{C}}_{[q+1]}) \equiv \mathbf{V}^{\mathrm{T}}(\mathbf{G}_{[q+1]}, \mathbf{C}_{[q+1]})\mathbf{V}$, $\widehat{\mathbf{b}}_{[q+1]} \equiv \mathbf{V}^{\mathrm{T}}\mathbf{b}_{[q+1]}$ and $\widehat{\mathbf{l}}_{[q+1]}(\lambda) \equiv \mathbf{V}^{\mathrm{T}}\mathbf{l}_{[q+1]}(\lambda)$. Although the order of the reduced system (12) is $p+1$ independent of q, the number of matched-moments is $(p+1)(q+1)$. This is an advantage of the CORE method. However, due to the geometric parameter λ appears in a power form of the reduced transfer function, it could lead to numerical instability, as illustrated in Section VI. Moreover, the reduced-order model does not preserve the structure of the original system. CORE is not a passivity-preserving scheme.

IV. PIMTAP Algorithm

To match the desired multiparameter moments as defined in (9), a natural choice of the projection subspace $\mathcal{V}$ is the subspace spanned by the corresponding moment generating vectors $\mathbf{r}_i^j$ defined by the recurrence (6)

$$\mathcal{V} = \text{span}\{\mathbf{r}_i^j : i = 0:p, j = 0:q\} \tag{13}$$

$$= \text{span}\begin{Bmatrix} \mathbf{r}_0^0, & \mathbf{r}_1^0, & \mathbf{r}_2^0, & \dots, & \mathbf{r}_p^0, \\ \mathbf{r}_0^1, & \mathbf{r}_1^1, & \mathbf{r}_2^1, & \dots, & \mathbf{r}_p^1, \\ \vdots & \vdots & \vdots & \vdots & \vdots \\ \mathbf{r}_0^q, & \mathbf{r}_1^q, & \mathbf{r}_2^q, & \dots, & \mathbf{r}_p^q. \end{Bmatrix} \tag{14}$$

where the horizontal direction is for frequency parameter s, and the vertical direction is for geometric parameter λ. A proof of the moment-matching property (9) using the projection subspace (13) is given in Appendix A. Note that the dimension n of the reduced-order system (7) is no greater than $(p+1)(q+1)$. It is smaller if deflations occur. See examples in Section VI.

The key question is how to stably and efficiently compute an orthonormal basis $\mathbf{V}$ of the subspace $\mathcal{V}$. The algorithm we propose in this section is to construct $\mathbf{V}$ incrementally in two directions as displayed in (14). If $\mathbf{V}_{j-1}$ is an orthonormal basis of the subspace spanned by the first $j-1$ rows of the vectors in the array (14), then to compute $\mathbf{V}_j$, we first form a basis $\mathbf{L}_j$ of the subspace spanned by the jth row vectors, i.e.,

$$\text{span}\{\mathbf{l}_j\} = \text{span}\left\{\mathbf{r}_0^{j-1}, \mathbf{r}_1^{j-1}, \dots, \mathbf{r}_p^{j-1}\right\} \tag{15}$$

and then combine $\mathbf{V}_{j-1}$ and $\mathbf{L}_j$, we have

$$\mathbf{V}_j = \text{orth}\left([\mathbf{V}_{j-1} \quad \mathbf{L}_j]\right) \tag{16}$$

where $\text{orth}(\mathbf{X})$ stands for an orthonormal basis of the range of $\mathbf{X}$. This process is done incrementally for $j = 2 : q+1$ and $\mathbf{V} = \mathbf{V}_{q+1}$.

Specifically, we first compute an orthonormal basis $\mathbf{V}_1$ of the subspace spanned by the first row vectors $\mathbf{r}_i^0$. By the recursion (6), the vectors $\mathbf{r}_i^0$ satisfy the linear recurrence

$$-\mathbf{G}_{[1]}\mathbf{r}_i^0 = \mathbf{C}_{[1]}\mathbf{r}_{i-1}^0, \qquad \text{for } i \geq 1$$

with $\mathbf{r}_0^0 = \mathbf{G}_0^{-1}\mathbf{b}$. Hence, the vectors $\mathbf{r}_i^0$ span the Krylov subspace $\mathcal{K}_{p+1}(\mathbf{A}_{[1]}, \mathbf{b}_{[1]})$, where $\mathbf{A}_{[1]} = -\mathbf{G}_{[1]}^{-1}\mathbf{C}_{[1]} \equiv -\mathbf{G}_0^{-1}\mathbf{C}_0$ and $\mathbf{b}_{[1]} = \mathbf{r}_0^0$. An orthonormal basis $\mathbf{V}_1$ of $\text{span}\{\mathbf{r}_i^0\}$ can be computed by the Arnoldi procedure [25].

We now consider how to compute the basis $\mathbf{L}_j$ for $j = 2 : q+1$. By stacking the vectors $\mathbf{r}_i^j$ columnwise and defining

$$\mathbf{r}_{[i]}^{[j]} = \begin{bmatrix} \mathbf{r}_{i-1}^0 \\ \mathbf{r}_{i-1}^1 \\ \vdots \\ \hline \mathbf{r}_{i-1}^{j-1} \end{bmatrix} \equiv \begin{bmatrix} \mathbf{r}_{[i]}^{[j-1]} \\ \hline \mathbf{r}_{i-1}^{j-1} \end{bmatrix}_N^{(j-1)N} \tag{17}$$

the two-directional recurrence (6) can be formally expressed by the following linear recurrence:

$$-\mathbf{G}_{[j]}\mathbf{r}_{[i]}^{[j]} = \mathbf{C}_{[j]}\mathbf{r}_{[i-1]}^{[j]}, \qquad \text{for } i > 1 \tag{18}$$

where $\mathbf{G}_{[j]}$ and $\mathbf{C}_{[j]}$ are jN by jN matrices of the forms

$$\mathbf{G}_{[j]} = \left[\begin{array}{cc|c} & & \\ & \mathbf{G}_{[j-1]} & \\ & & \\ \hline \mathbf{0} & \mathbf{G}_1 & \mathbf{G}_0 \end{array}\right] \quad \mathbf{C}_{[j]} = \left[\begin{array}{cc|c} & & \\ & \mathbf{C}_{[j-1]} & \\ & & \\ \hline \mathbf{0} & \mathbf{C}_1 & \mathbf{C}_0 \end{array}\right]. \tag{19}$$

The initial vector is $\mathbf{r}_{[1]}^{[j]} = \mathbf{G}_{[j]}^{-1}\begin{bmatrix} \mathbf{b} \\ \mathbf{0} \end{bmatrix}$.

To verify the recurrence (18), let us first write it explicitly for $j = 2$

$$-\begin{bmatrix} \mathbf{G}_0 & \\ \mathbf{G}_1 & \mathbf{G}_0 \end{bmatrix}\begin{bmatrix} \mathbf{r}_i^0 \\ \mathbf{r}_i^1 \end{bmatrix} = \begin{bmatrix} \mathbf{C}_0 & \\ \mathbf{C}_1 & \mathbf{C}_0 \end{bmatrix}\begin{bmatrix} \mathbf{r}_{i-1}^0 \\ \mathbf{r}_{i-1}^1 \end{bmatrix}.$$

Hence, we have

$$-\mathbf{G}_0\mathbf{r}_i^0 = \mathbf{C}_0\mathbf{r}_{i-1}^0$$
$$-\mathbf{G}_0\mathbf{r}_i^1 = \mathbf{C}_0\mathbf{r}_{i-1}^1 + \mathbf{G}_1\mathbf{r}_i^0 + \mathbf{C}_1\mathbf{r}_{i-1}^0.$$

By inverting the matrix $\mathbf{G}_0$, we immediately have the recursion (6) for $j = 0$ and $j = 1$, respectively. In general, by the definition (19) of the matrices $\mathbf{G}_{[j]}$ and $\mathbf{C}_{[j]}$, we have

$$-\mathbf{G}_0\mathbf{r}_i^{j-1} = \mathbf{C}_0\mathbf{r}_{i-1}^{j-1} + \mathbf{G}_1\mathbf{r}_i^{j-1} + \mathbf{C}_1\mathbf{r}_{i-1}^{j-2}$$

which immediately leads to the two-directional recurrence (6) by inverting the matrix $\mathbf{G}_0$.

The linear recurrence (18) suggests that the vectors $\mathbf{r}_{[i]}^{[j]}$ span the Krylov subspace

$$\text{span}\left\{\mathbf{r}_{[1]}^{[j]}, \mathbf{r}_{[2]}^{[j]}, \dots, \mathbf{r}_{[p+1]}^{[j]}\right\} = \mathcal{K}_{p+1}\left(\mathbf{A}_{[j]}, \mathbf{b}_{[\mathbf{j}]}\right)$$

where $\mathbf{A}_{[j]} = -\mathbf{G}_{[j]}^{-1}\mathbf{C}_{[j]}$ and $\mathbf{b}_{[j]} = \mathbf{r}_{[1]}^{[j]}$.

We have two ways to generate the basis matrix $\mathbf{L}_j$. One is to apply the Arnoldi procedure with $\mathbf{A}_{[j]}$ and $\mathbf{b}_{[j]}$ to obtain

an orthonormal basis $\mathbf{Q}_{p+1}^{[j]}$ of $\mathcal{K}_{p+1}(\mathbf{A}_{[j]}, \mathbf{b}_{[j]})$. Let $\mathbf{Q}_{p+1}^{[j]}$ be partitioned into

$$\mathbf{Q}_{p+1}^{[j]} = \begin{bmatrix} \widetilde{\mathbf{Q}}_1 \\ \widetilde{\mathbf{Q}}_2 \end{bmatrix}_N^{(j-1)N}. \tag{20}$$

Then, we have

$$\text{span}\{\widetilde{\mathbf{Q}}_2\} = \text{span}\{\mathbf{L}_j\}. \tag{21}$$

Alternatively, we can exploit the relation between Krylov subspaces $\mathcal{K}_{p+1}(\mathbf{A}_{[j-1]}, \mathbf{b}_{[j-1]})$ and $\mathcal{K}_{p+1}(\mathbf{A}_{[j]}, \mathbf{b}_{[j]})$ and *directly* compute the basis matrix $\mathbf{L}_j$. We note that $\mathbf{A}_{[j]}$ and $\mathbf{b}_{[j]}$ are the bordered matrix and vector of $\mathbf{A}_{[j-1]}$ and $\mathbf{b}_{[j-1]}$

$$\mathbf{A}_{[j]} = \begin{bmatrix} \mathbf{A}_{[j-1]} & \\ \mathbf{A}_{[j,:]} & \mathbf{A}_j \end{bmatrix} \quad \mathbf{b}_{[j]} = \begin{bmatrix} \mathbf{b}_{[j-1]} \\ \mathbf{b} \end{bmatrix} \tag{22}$$

where

$$\begin{aligned} \mathbf{A}_{[j+1,:]} &= -\mathbf{G}_0^{-1}\left([\mathbf{0} \quad \mathbf{G}_1]\mathbf{A}_{[j]} + [\mathbf{0} \quad \mathbf{C}_1]\right) \\ \mathbf{A}_{j+1} &= -\mathbf{G}_0^{-1}\mathbf{C}_0 \\ \mathbf{b}_j &= \mathbf{r}_0^{j-1} = -\mathbf{G}_0^{-1}[\mathbf{0} \quad \mathbf{G}_1]\mathbf{b}_{[j-1]}. \end{aligned}$$

If $\mathbf{Q}_{p+1}^{[j]}$ is an orthonormal basis of $\mathcal{K}_{p+1}(\mathbf{A}_{[j]}, \mathbf{b}_{[j]})$ and is partitioned as in (20), then we have the following two facts:

1) $\text{span}\{\mathbf{r}_{[1]}^{[j-1]}, \mathbf{r}_{[2]}^{[j-1]}, \ldots, \mathbf{r}_{[p+1]}^{[j-1]}\} = \text{span}\{\widetilde{\mathbf{Q}}_1\}$.
2) $\text{span}\{\mathbf{r}_0^{j-1}, \mathbf{r}_1^{j-1}, \ldots, \mathbf{r}_p^{j-1}\} = \text{span}\{\widetilde{\mathbf{Q}}_2\}$.

Fact 1) is due to the relation (22). Fact 2) is given by the same argument used for (21). Therefore, $\mathbf{Q}_{p+1}^{[j]}$ can be written in the form

$$\mathbf{Q}_{p+1}^{[j]} = \begin{bmatrix} \mathbf{Q}_{p+1}^{[j-1]}\mathbf{R}_j \\ \mathbf{L}_j \end{bmatrix} \tag{23}$$

where $\mathbf{R}_j$ is upper triangular and $\mathbf{L}_j$ satisfies the property (15). Subsequently, we can use the relation (23) and directly compute $\mathbf{L}_j$. Such a computational procedure is given in Appendix B and is referred to as a TAP.

Once the basis $\mathbf{L}_j$ is available, an orthonormal basis matrix $\mathbf{V}_j$ is computed by (16). Note that $\mathbf{V}_{j-1}$ is already orthonormal, there is an efficient method [26] to compute $\mathbf{V}_j$. The following outline is a summary to compute the reduced system (7) satisfying the moment-matching property (9):

PIMTAP ALGORITHM

1) Run the Arnoldi algorithm with $\mathbf{A}_{[1]}$ and $\mathbf{b}_{[1]}$ to construct the orthonormal basis $\mathbf{V}_1 \equiv \mathbf{Q}_{p+1}^{[1]}$.
2) For $j = 2, 3, \ldots, q+1$,
   a) Run the TAP (Appendix B) with $\mathbf{A}_{[j,:]}$, $\mathbf{A}_j$ and $\mathbf{b}_j$ to construct the basis matrix $\mathbf{L}_j$.
   b) $\mathbf{V}_j = \text{orth}([\mathbf{V}_{j-1} \quad \mathbf{L}_j])$.
3) Set $\mathbf{V} = \mathbf{V}_{q+1}$.
4) Compute the reduced-order model (7).

A few remarks are in order: The PIMTAP is a stable process since the TAP stably generates the basis matrix $\mathbf{L}_j$. Meanwhile the PIMTAP model has the same form of the original system (3) and preserves important properties such as passivity and stability. Furthermore, the PIMTAP is an adaptive process with respect to the approximation orders of geometric and/or frequency parameters since the TAP incrementally generates the basis matrix $\mathbf{L}_j$. This will be shown in Example C in Section VI.

V. PIMTAP FOR MULTIPARAMETER SYSTEMS

In this section, we extend the PIMTAP for the multiparameter affine linear system (1) and (2). It is sufficient to just consider two-parameter $\lambda = (\lambda_1, \lambda_2)$. The pattern for general k should be clear. The transfer function $h(s, \lambda)$ is given by

$$h(s,\lambda) = \mathbf{l}^{\mathrm{T}}\left(\mathbf{G}_0 + \sum_{i=1}^{2}\lambda_i\mathbf{G}_i + s\left(\mathbf{C}_0 + \sum_{i=1}^{2}\lambda_i\mathbf{C}_i\right)\right)^{-1}\mathbf{b}. \tag{24}$$

Let us define a *multiindex* $\alpha = (\alpha_1, \alpha_2)$, where α_1 and α_2 are nonnegative integers. $|\alpha| = \alpha_1 + \alpha_2$ is the *order* of α. The monomial λ^α is defined by $\lambda^\alpha = \lambda_1^{\alpha_1}\lambda_2^{\alpha_2}$. Following [27], a power series expansion of (24) can be formally written as

$$h(s,\lambda) = \sum_{|\alpha|=0}^{\infty}\sum_{i=0}^{\infty} m_i^\alpha s^i \lambda^\alpha$$

where $m_i^\alpha = \mathbf{l}^{\mathrm{T}}\mathbf{r}_i^\alpha$ are (multiparameter) moments and the vectors $\mathbf{r}_i^\alpha = \mathbf{r}_i^{\alpha_1,\alpha_2}$ are defined by the following recursion:

$$\begin{aligned} \mathbf{r}_i^{\alpha_1,\alpha_2} = -\mathbf{G}_0^{-1}\Big(&\mathbf{G}_1\mathbf{r}_i^{\alpha_1-1,\alpha_2} + \mathbf{G}_2\mathbf{r}_i^{\alpha_1,\alpha_2-1} \\ &+ \mathbf{C}_0\mathbf{r}_{i-1}^{\alpha_1,\alpha_2} + \mathbf{C}_1\mathbf{r}_{i-1}^{\alpha_1-1,\alpha_2} + \mathbf{C}_2\mathbf{r}_{i-1}^{\alpha_1,\alpha_2-1}\Big) \end{aligned} \tag{25}$$

with $\mathbf{r}_0^{0,0} = \mathbf{G}_0^{-1}\mathbf{b}$ and $\mathbf{r}_i^{\alpha_1,\alpha_2} = \mathbf{0}$ if α_1, α_2 or i is negative.

Given desired approximation orders p and q of frequency and geometric parameters s and λ, respectively, we seek a projection subspace $\mathcal{V}$ that produces a reduced-order system satisfying the following moment-matching property:

$$m_i^\alpha = \widehat{m}_i^\alpha, \qquad i = 0:p, |\alpha| = 0; q. \tag{26}$$

The total number of the matched moments is $(p+1)(q+2)(q+1)/2$. This implies that

$$\begin{aligned} h(s,\lambda) - \widehat{h}(s,\lambda) = &\underbrace{\sum_{i=p+1}^{\infty}\left(\sum_{|\alpha|=0}^{q}\left(m_i^\alpha - \widehat{m}_i^\alpha\right)\lambda^\alpha\right)s^i}_{\mathcal{O}(s^{p+1})} \\ &+ \underbrace{\sum_{|\alpha|=q+1}^{\infty}\left(\sum_{i=0}^{\infty}\left(m_i^\alpha - \widehat{m}_i^\alpha\right)s^i\right)\lambda^\alpha}_{\mathcal{O}(\lambda^{q+1})}. \end{aligned}$$

To match the desired multiparameter moments as defined in (26), a choice of the projection subspace $\mathcal{V}$ is as the following:

$$\mathcal{V} = \text{span}\{\mathbf{r}_i^\alpha : i = 0:p, |\alpha| = 0:q\} \tag{27}$$

$$= \text{span}\left\{\begin{matrix} \mathbf{r}_0^{0,0}, & \mathbf{r}_1^{0,0}, & \mathbf{r}_2^{0,0}, & \ldots, & \mathbf{r}_p^{0,0} \\ \mathbf{r}_0^{1,0}, & \mathbf{r}_1^{1,0}, & \mathbf{r}_2^{1,0}, & \ldots, & \mathbf{r}_p^{1,0}, \\ \mathbf{r}_0^{0,1}, & \mathbf{r}_1^{0,1}, & \mathbf{r}_2^{0,1}, & \ldots, & \mathbf{r}_p^{0,1}, \\ \vdots & \vdots & \vdots & \vdots & \vdots \\ \mathbf{r}_0^{0,q}, & \mathbf{r}_1^{0,q}, & \mathbf{r}_2^{0,q}, & \ldots, & \mathbf{r}_p^{0,q}. \end{matrix}\right\} \tag{28}$$

where the horizontal direction is for frequency parameter s, and the vertical direction is for geometric parameter λ, ordered by $|\alpha| = 0 : q$, The vectors $\{\mathbf{r}_0^\alpha, \mathbf{r}_1^\alpha, \ldots, \mathbf{r}_p^\alpha : |\alpha| = 0\}$ constitute the first row. The vectors $\{\mathbf{r}_0^\alpha, \mathbf{r}_1^\alpha, \ldots, \mathbf{r}_p^\alpha : |\alpha| = 1\}$ constitute the second and third rows, and so on. The moment-matching property can be shown by an analogous argument in Appendix A.

For the question of stably and efficiently generate an orthonormal basis $\mathbf{V}$ of the projection subspace $\mathcal{V}$, in analogy to the case of single parameter, we can incrementally construct $\mathbf{V}$ in two directions. If $\mathbf{V}_j$ is an orthonormal basis of the subspace spanned by $\mathbf{r}_i^\alpha$ of the first $j(j+1)/2$ rows of (28), then for computing $\mathbf{V}_j$, we first form a basis $\mathbf{L}_j$ such that

$$\text{span}\left\{\mathbf{L}_j = \begin{bmatrix}\widetilde{\mathbf{L}}_1 \\ \widetilde{\mathbf{L}}_2 \\ \vdots \\ \widetilde{\mathbf{L}}_j\end{bmatrix}\right\} = \text{span}\left\{\begin{bmatrix}\mathbf{r}_i^{j-1,0} \\ \mathbf{r}_i^{j-2,1} \\ \vdots \\ \mathbf{r}_i^{0,j-1}\end{bmatrix} \;:\; i = 0 : p\right\}$$

and then reshape $\mathbf{L}_j$ to define $\mathbf{X}_j$

$$\mathbf{X}_j = \text{reshape}(\mathbf{L}_j) \equiv [\widetilde{\mathbf{L}}_1 \quad \widetilde{\mathbf{L}}_2 \quad \ldots \quad \widetilde{\mathbf{L}}_j]. \tag{29}$$

It is easy to see that

$$\text{span}\{\mathbf{X}_j\} = \text{span}\left\{\mathbf{r}_0^\alpha, \ldots, \mathbf{r}_p^\alpha : |\alpha| = j-1\right\}. \tag{30}$$

We then combine $\mathbf{V}_{j-1}$ and $\mathbf{X}_j$ to obtain an orthonormal basis

$$\mathbf{V}_j = \text{orth}\left([\mathbf{V}_{j-1} \quad \mathbf{X}_j]\right). \tag{31}$$

The procedure is carried iteratively for $j = 2 : q+1$ and $\mathbf{V} = \mathbf{V}_{q+1}$.

To build an orthonormal basis $\mathbf{V}_1$ of the subspace spanned by the first row vectors $\mathbf{r}_i^{0,0}$ of (28), we observe the vectors $\mathbf{r}_i^{0,0}$ satisfy the linear recurrence

$$\mathbf{r}_i^{0,0} = \mathbf{A}_{[1]}\mathbf{r}_{i-1}^{0,0}, \qquad \text{for } i \geq 1$$

where $\mathbf{A}_{[1]} = -\mathbf{G}_0^{-1}\mathbf{C}_0$ and $\mathbf{r}_0^{0,0} = \mathbf{G}_0^{-1}\mathbf{b}$. Consequently, the vectors of the first row span the Krylov subspace $\mathcal{K}_{p+1}(\mathbf{A}_{[1]}, \mathbf{b}_{[1]})$, where $\mathbf{b}_{[1]} = \mathbf{r}_0^{0,0}$. An orthonormal basis $\mathbf{V}_1$ of $\mathcal{K}_{p+1}(\mathbf{A}_{[1]}, \mathbf{b}_{[1]})$ can be obtained by the Arnoldi procedure.

We now consider how to compute $\mathbf{L}_2$, $\mathbf{L}_3, \ldots, \mathbf{L}_{q+1}$ and reshape them to obtain $\mathbf{X}_2$, $\mathbf{X}_3, \ldots, \mathbf{X}_{q+1}$. In order to obtain a basis $\mathbf{X}_j$ of the subspace

$$\text{span}\left\{\mathbf{r}_0^\alpha, \mathbf{r}_1^\alpha, \ldots, \mathbf{r}_p^\alpha : |\alpha| = j-1\right\}$$

we first define a linear ordering of the set $\{\alpha = (\alpha_1, \alpha_2) : |\alpha| = 0, 1, 2, \ldots\}$ as the following:

$$\begin{aligned}&(0,0),\\ &(1,0),\ (0,1),\\ &(2,0),\ (1,1),\ (0,2),\\ &\quad\vdots\\ &(j,0),\ (j-1,1), \ldots, (1,j-1),\ (0,j).\end{aligned} \tag{32}$$

In other words, the pair (α_1, α_2) is mapped to the $k(\alpha_1, \alpha_2)$th term in the linear ordering (32), where $k(\alpha_1, \alpha_2) = (1/2)(\alpha_1 + \alpha_2 + 1)(\alpha_1 + \alpha_2) + \alpha_2 + 1$. Correspondingly, the vectors $\mathbf{r}_i^\alpha$ are ordered according to the sequence (32). Let the vector $\mathbf{r}_{[i]}^{[j]}$ of the length $j(j+1)N/2$ be defined through stacking the vectors $\mathbf{r}_{\mathbf{i-1}}^\alpha$ in the same order

$$\mathbf{r}_{[i]}^{[j]} = \begin{bmatrix}\mathbf{r}_{i-1}^{0,0} \\ \mathbf{r}_{i-1}^{1,0} \\ \mathbf{r}_{i-1}^{0,1} \\ \vdots \\ \hline \mathbf{r}_{i-1}^{j-1,0} \\ \mathbf{r}_{i-1}^{j-2,1} \\ \vdots \\ \mathbf{r}_{i-1}^{0,j-1}\end{bmatrix} \equiv \begin{bmatrix}\mathbf{r}_{[i]}^{[j]} \\ \hline \mathbf{r}_{i-1}^{j-1,0} \\ \mathbf{r}_{i-1}^{j-2,1} \\ \vdots \\ \mathbf{r}_{i-1}^{0,j-1}\end{bmatrix}.$$

Then, similarly to (18), we have the linear recurrence

$$\mathbf{r}_{[i]}^{[j]} = \mathbf{A}_{[j]}\mathbf{r}_{[i-1]}^{[j]}, \qquad \text{for } i > 1 \tag{33}$$

where the coefficient matrix and the initial vector are

$$\mathbf{A}_{[j]} = -\mathbf{G}_{[j]}^{-1}\mathbf{C}_{[j]} \quad \mathbf{r}_{[1]}^{[j]} = \mathbf{G}_{[j]}^{-1}\begin{bmatrix}\mathbf{b} \\ \mathbf{0}\end{bmatrix} \equiv \mathbf{b}_{[j]} \tag{34}$$

$\mathbf{G}_{[j]}$ and $\mathbf{C}_{[j]}$ square matrices of size $j(j+1)N/2$

$$\boldsymbol{\Delta}_{[j]} = \begin{bmatrix}\boldsymbol{\Delta}_{[j-1]} & \\ \boldsymbol{\Delta}_{[j,:]} & \mathbf{I}_j \otimes \boldsymbol{\Delta}_0\end{bmatrix}, \qquad \boldsymbol{\Delta} \in \{\mathbf{G}, \mathbf{C}\}.$$

The operator $\otimes$ denotes the Kronecker product. The sub-matrices $\mathbf{G}_{[j,:]}$ and $\mathbf{C}_{[j,:]}$ are jN by $(j-1)jN/2$ defined by

$$\boldsymbol{\Delta}_{[j,:]} = \left[\begin{array}{c|cccc}\mathbf{0} & \boldsymbol{\Delta}_1 & & & \\ \mathbf{0} & \boldsymbol{\Delta}_2 & \boldsymbol{\Delta}_1 & & \\ \vdots & & \boldsymbol{\Delta}_2 & \ddots & \\ & & & \ddots & \boldsymbol{\Delta}_1 \\ \mathbf{0} & & & & \boldsymbol{\Delta}_2 \\ \mathbf{0} & & & & \end{array}\right], \qquad \boldsymbol{\Delta} \in \{\mathbf{G}, \mathbf{C}\}$$

where the size of zero column is $[(j-1)j/2 - (j-1)]N$. By the recurrence (33), the vectors $\mathbf{r}_{[i]}^{[j]}$ span the Krylov subspace

$$\text{span}\left\{\mathbf{r}_{[1]}^{[j]}, \mathbf{r}_{[2]}^{[j]}, \ldots, \mathbf{r}_{[p+1]}^{[j]}\right\} = \mathcal{K}_{p+1}\left(\mathbf{A}_{[j]}, \mathbf{b}_{[j]}\right).$$

Since the matrix $\mathbf{A}_{[j]}$ and the vector $\mathbf{b}_{[j]}$ are the bordered matrix and vector of $\mathbf{A}_{[j-1]}$ and $\mathbf{b}_{[j-1]}$, respectively,

$$\mathbf{A}_{[j]} = \begin{bmatrix}\mathbf{A}_{[j-1]} & \\ \mathbf{A}_{[j,:]} & \mathbf{A}_j\end{bmatrix}, \quad \mathbf{b}_{[j]} = \begin{bmatrix}\mathbf{b}_{[j-1]} \\ \mathbf{b}_j\end{bmatrix}$$

where

$$\begin{aligned}\mathbf{A}_{[j,:]} &= -\left(\mathbf{I}_j \otimes \mathbf{G}_0^{-1}\right)\left(\mathbf{G}_{[j,:]}\mathbf{A}_{[j-1]} + \mathbf{C}_{[j,:]}\right)\\ \mathbf{A}_j &= -\left(\mathbf{I}_j \otimes \mathbf{G}_0^{-1}\right)\left(\mathbf{I}_j \otimes \mathbf{C}_0\right)\\ \mathbf{b}_j &= -\left(\mathbf{I}_j \otimes \mathbf{G}_0^{-1}\right)\left(\mathbf{G}_{[j,:]}\mathbf{b}_{[j-1]}\right).\end{aligned}$$

By the same argument for (23), an orthonormal basis $\mathbf{Q}_{p+1}^{[j]}$ of $\mathcal{K}_{p+1}(\mathbf{A}_{[j]}, \mathbf{b}_{[j]})$ can be written in the form

$$\mathbf{Q}_{p+1}^{[j]} = \begin{bmatrix} \mathbf{Q}_{p+1}^{[j-1]} \mathbf{R}_j \\ \mathbf{L}_j \end{bmatrix}$$

where $\mathbf{R}_j$ is upper triangular and

$$\text{span}\{\mathbf{L}_j\} = \text{span}\left\{ \begin{bmatrix} \mathbf{r}_i^{j-1,0} \\ \mathbf{r}_i^{j-2,1} \\ \vdots \\ \mathbf{r}_i^{0,j-1} \end{bmatrix} : i = 0, 1, 2, \ldots, p \right\}.$$

Therefore, we can apply the TAP (see Appendix B) to directly compute the matrices $\mathbf{R}_j$ and $\mathbf{L}_j$. Subsequently, after reshaping the matrix $\mathbf{L}_j$ by (29), we obtain the basis matrix $\mathbf{X}_j$ of the subspace (30). An orthonormal basis $\mathbf{V}_j$ of the subspace spanned by the vectors in the first $j(j+1)/2$ rows of the vector array (28) is computed by (31).

In summary, the procedure for systems of multiple geometric parameters is similar to the single geometric parameter case with the following two additional steps.

1) Order the vectors $\mathbf{r}_i^{\alpha}$ in the sequence as in (32).
2) Reshape the matrix $\mathbf{L}_j$ to get the matrix $\mathbf{X}_j$ as in (29).

The computational complexity of the PIMTAP for the affine linear system (1) and (2) of k geometric parameters can be characterized by the number of basis vectors $\mathbf{r}_i^{\alpha}$ of the projection subspace $\mathcal{V}$. For simplicity, assume that all geometric parameters are of the same order q of approximation, and the approximation order of the frequency parameter s is p. Then, by a straightforward calculation, the dimension of $\mathcal{V}$ is

$$n(k, p, q) = (p+1)C_k^{q+k} \tag{35}$$

where $C_m^n = (n!/(n-m)!n!)$ is the binomial coefficient. $n(k, p, q)$ grows exponentially. This is known as the *curse of dimensionality* for all moment-matching-based PMOR methods.

VI. Numerical Results

In this section, we present three numerical examples to demonstrate the accuracy, stability and efficiency of the proposed PIMTAP algorithm. All experiments are conducted in MATLAB and run on a PC with a 1.6-GHz Intel Core Duo T2050 processor.

EXAMPLE A. We consider an interconnect circuit consisting of an 8-bit bus and two shielding lines from an industrial application (see Fig. 2). The near end of the first line is driven by a current source as the excitation and the voltage of node A is regarded as the output signal. An RLC modified nodal analysis formulation is used to model the capacitive and magnetic coupling effects between any two of these lines. The description matrices are

$$\mathbf{C}(\lambda) = \begin{bmatrix} (1+\lambda)\mathbf{Q} & \mathbf{0} \\ \mathbf{0} & \mathbf{H} \end{bmatrix} \quad \mathbf{G}(\lambda) = \begin{bmatrix} (1+\lambda)\mathbf{N} & \mathbf{E} \\ -\mathbf{E}^{\mathrm{T}} & \mathbf{0} \end{bmatrix}$$

where $\mathbf{Q}$, $\mathbf{H}$, and $\mathbf{N}$ are capacitance, inductance, and resistance matrices, respectively. $\mathbf{E}$ is the incident matrix associated with the inductive connectivity. λ represents the fabrication variation and is assumed to be varied within $\pm 15\%$. The order of $\mathbf{Q}$ and $\mathbf{N}$ is 330 and the order of $\mathbf{H}$ is 160.

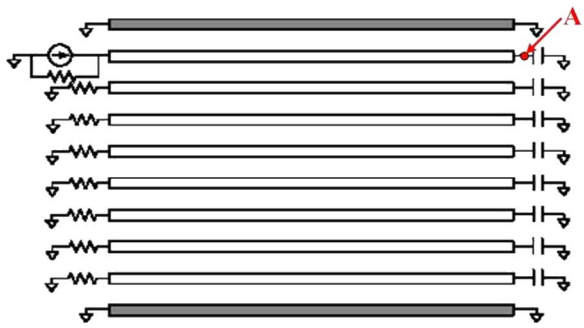

Fig. 2. Eight-bit bus system with two shield lines.

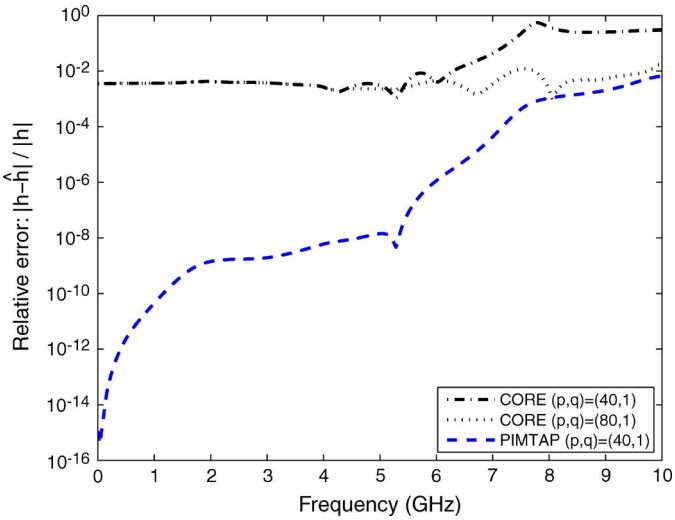

Fig. 3. Relative errors of the PIMTAP and the CORE models.

Fig. 3 shows the relative errors of the transfer functions computed by the CORE and the PIMTAP at $\lambda = 0.06$. It clearly shows that the PIMTAP model with $(p, q) = (40, 1)$ is more accurate than the CORE model with $(p, q) = (80, 1)$. The order of the PIMTAP model is 76 instead of 82, due to the deflations among the basis vectors $\mathbf{r}_i^j$. The order of the CORE model is 81.

To improve the approximation accuracy, we increase the approximation order q of λ. Fig. 4 shows that the CORE model becomes unstable at high frequencies. On the other hand, the PIMTAP model is stable, and its curve is visually indistinguishable from the original one.

Fig. 5 shows that the PIMTAP model captures the frequency response at three different geometric parameters. The maximum relative error is smaller than $\mathcal{O}(10^{-2})$ on the frequency range [0, 10] GHz for all selected points of the geometric parameter λ in the interval $[-0.15, 0.15]$.

Finally, to compare the CPU elapsed time, we partition the interval $[-0.15, 0.15]$ of λ into ten equal length subintervals and the frequency range [0, 10] GHz into 300 equal length subintervals. Thus, we have 11×301 grid points (λ_k, s_ℓ). Table I shows the approximation orders (p, q), dimensions of the reduced-order systems, maximum relative errors and

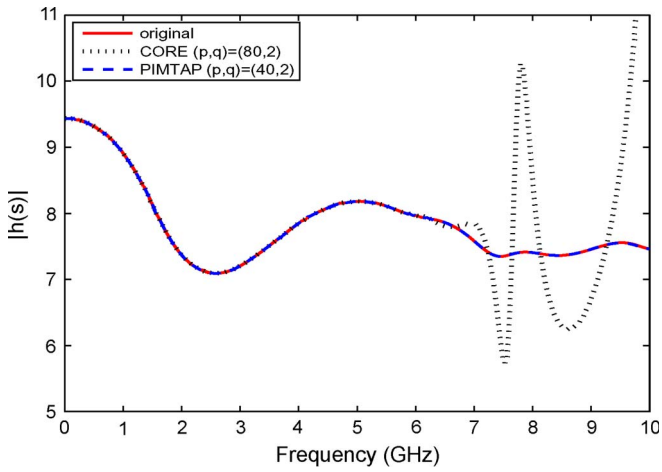

Fig. 4. Frequency responses for $\lambda = 0.06$.

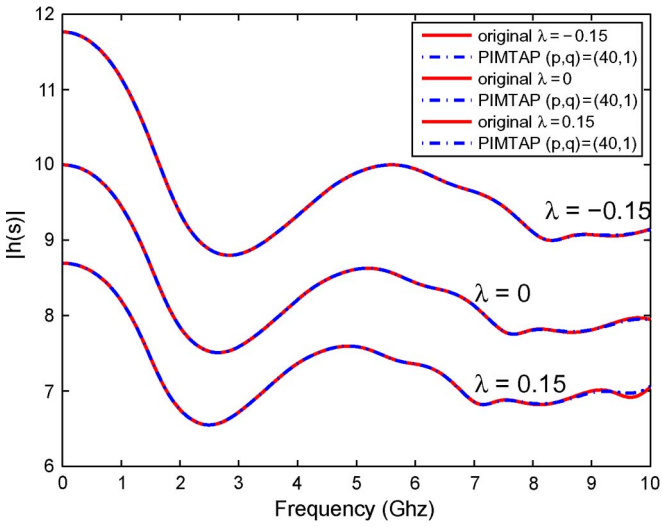

Fig. 5. Frequency responses for $\lambda = -0.15, 0, 0.15$.

TABLE I
COMPARISON OF PIMTAP AND CORE

	CORE		PIMTAP
(p, q)	(40,1)	(80,1)	(40,1)
Reduced-order n	41	81	76
Max relative-error	$\mathcal{O}(10^0)$	$\mathcal{O}(10^{-2})$	$\mathcal{O}(10^{-2})$
CPU-pmor (s)	0.594	1.859	0.453
CPU-tfcal (s)	1.984	8.641	6.719
CPU-total (s)	2.578	10.490	7.172

CPU elapsed time. CPU-pmor is the time for constructing the reduced-order model including generating an orthonormal basis $\mathbf{V}$ of the projection subspace. CPU-tfcal is the time for calculating the transfer functions at all 11×301 points (λ_k, s_ℓ). Note that the CORE model with $(p, q) = (40, 1)$ theoretically matches the same number of moments as the PIMTAP model with $(p, q) = (40, 1)$. The orders of the CORE and the PIMTAP models are 41 and 76, respectively. Hence, the CPU-tfcal of the CORE model is smaller than the PIMTAP model. However, its accuracy is poor. To have a comparable accuracy, the CORE needs to take $(p, q) = (80, 1)$. Subsequently, the order of the CORE model is 81 and takes more time (CPU-tfcal) for transfer function evaluations.

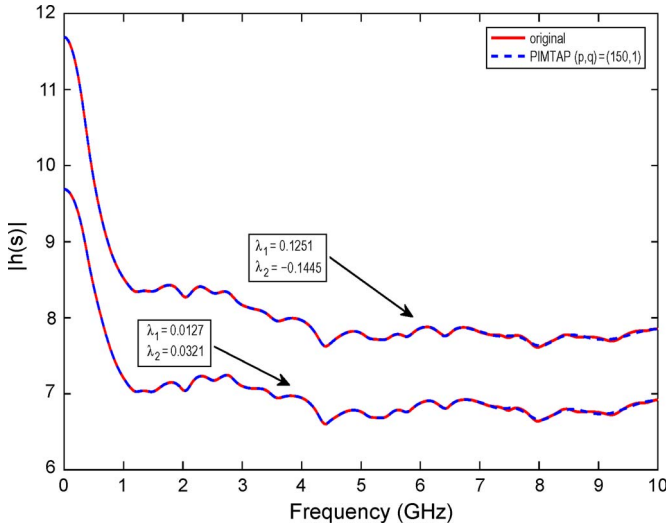

Fig. 6. Frequency responses at selected pairs (λ_1, λ_2).

TABLE II
MAXIMUM RELATIVE ERRORS AT SELECTED POINTS

λ_1	λ_2	max rel.-err
3.46%	13.51%	5.2647×10^{-3}
8.76%	-8.06%	4.0396×10^{-3}
12.65%	3.21%	4.3783×10^{-3}
7.14%	-0.42%	4.2621×10^{-3}
-9.71%	11.74%	5.3467×10^{-3}
-2.82%	7.86%	4.9821×10^{-3}
13.06%	-1.31%	4.1319×10^{-3}
12.51%	-14.45%	3.7567×10^{-3}
-2.68%	9.64%	5.1238×10^{-3}
1.18%	-1.65%	4.1313×10^{-3}

TABLE III
COMPARISON OF PIMTAP AND CORE

(p, q)	(150,1)	(450,1)	(150,1)
Reduced-order n	151	451	362
Max rel.-error	1.71×10^{-1}	1.16×10^{-1}	10^{-3}
CPU-pmor (s)	24.67	214.46	23.57
CPU-tfcal (s)	41.12	741.47	365.34
CPU-total (s)	65.79	955.93	388.91

EXAMPLE B. We consider an RLC network with two geometric parameters. The description matrices are

$$\mathbf{C}(\lambda) = \begin{bmatrix} (1+\lambda_1)\mathbf{Q} & \mathbf{0} \\ \mathbf{0} & \mathbf{H} \end{bmatrix} \quad \mathbf{G}(\lambda) = \begin{bmatrix} (1+\lambda_2)\mathbf{N} & \mathbf{E} \\ -\mathbf{E}^{\mathrm{T}} & \mathbf{0} \end{bmatrix}$$

where λ_1 and λ_2 represent variations in capacitance $\mathbf{Q}$ and resistance $\mathbf{N}$, respectively. The order of $\mathbf{Q}$ nd $\mathbf{N}$ is 1222, and the order of $\mathbf{H}$ is 544.

Fig. 6 shows that the PIMTAP model with approximation order $(p, q) = (150, 1)$ is visually indistinguishable from the exact transfer function. Due to the deflations, the order of the reduce PIMTAP model is 362. The number of matched moments is $(150 + 1)(1 + 2)(1 + 1)/2 = 453$. The maximum relative errors on the frequency range [0, 10] GHz of the reduced-order PIMTAP models for ten selected pairs (λ_1, λ_2) are presented in Table II. Table III compares the performance of the PIMTAP and the CORE methods. It includes the approximation order (p, q), dimension of a reduced-order model, maximum relative errors, and profiles of CPU at ten

selected pairs of (λ_1, λ_2) specified in Table II. We note that even with the approximation order (450, 1), the accuracy of the CORE model is still worse than the PIMTAP due to the truncation error of the CORE model.

EXAMPLE C. In this example, we consider a multiparameter model from a joint electrothermal simulation of a MEMS device [23]. After discretization in space by a finite element analysis of the heat transfer, we have a three-parameter linear system of the form

$$\begin{cases} \mathbf{E}\dot{\mathbf{t}}(t) + \left(\mathbf{K} + \sum\limits_{i\in\{t,s,b\}} \lambda_i \mathbf{K}_i\right)\mathbf{t}(t) = \mathbf{b}u(t) \\ \mathbf{y}(t) = \mathbf{C}^{\mathrm{T}}\mathbf{t}(t) \end{cases} \tag{36}$$

where $\mathbf{t}(t)$ is the vector of unknown temperatures, and $\mathbf{E}$ and $\mathbf{K}$ are matrices representing the heat capacity and conductivity. λ_{t}, λ_{s}, and λ_{b} are film coefficients describing the heat flow between the device and three boundaries (top, side, and bottom), respectively. The matrices $\mathbf{K}_{\mathrm{t}}$, $\mathbf{K}_{\mathrm{s}}$, and $\mathbf{K}_{\mathrm{b}}$ specify the contributions of the film coefficients to the global system matrix $\mathbf{K}$. $u(t)$ is the heat source. Here, $\mathbf{b}$ is a column vector and $\mathbf{C}$ is an $N \times 7$ output matrix, where the order N of the system is $N = 4257$.

Following [23], we consider an expansion of the transfer function $\mathbf{h}(s, \lambda)$ of the system (36) at the point $(s, \lambda_{\mathrm{t}}, \lambda_{\mathrm{s}}, \lambda_{\mathrm{b}}) = (0, 10, 10, 10)$

$$\begin{aligned} \mathbf{h}(s,\lambda) &= \mathbf{C}^{\mathrm{T}}(\mathbf{K} + \lambda_{\mathrm{t}}\mathbf{K}_{\mathrm{t}} + \lambda_{\mathrm{s}}\mathbf{K}_{\mathrm{s}} + \lambda_{\mathrm{b}}\mathbf{K}_{\mathrm{b}} + s\mathbf{E})^{-1}\mathbf{b} \\ &= \sum_{|\alpha|=0}^{\infty}\sum_{i=0}^{\infty}\left(\mathbf{C}^{\mathrm{T}}\mathbf{r}_i^{\alpha}\right)s^i\widetilde{\lambda}^{\alpha} \end{aligned}$$

where $\widetilde{\boldsymbol{\lambda}} = (\widetilde{\lambda}_{\mathrm{t}}, \widetilde{\lambda}_{\mathrm{s}}, \widetilde{\lambda}_{\mathrm{b}}) = (\lambda_{\mathrm{t}} - 10, \lambda_{\mathrm{s}} - 10, \lambda_{\mathrm{b}} - 10)$. α is a multiindex $\alpha = (\alpha_{\mathrm{t}}, \alpha_{\mathrm{s}}, \alpha_{\mathrm{b}})$, where α_{t}, α_{s}, and α_{b} are nonnegative integers. The moment generating vectors $\mathbf{r}_i^{\alpha}$ are defined by the recurrence

$$\begin{aligned} \mathbf{r}_i^{\alpha} = \mathbf{r}_i^{\alpha_{\mathrm{t}},\alpha_{\mathrm{s}},\alpha_{\mathrm{b}}} = -\widetilde{\mathbf{K}}^{-1}\Big(&\mathbf{K}_{\mathrm{t}}\mathbf{r}_i^{\alpha_{\mathrm{t}}-1,\alpha_{\mathrm{s}},\alpha_{\mathrm{b}}} + \mathbf{K}_{\mathrm{s}}\mathbf{r}_i^{\alpha_{\mathrm{t}},\alpha_{\mathrm{s}}-1,\alpha_{\mathrm{b}}} \\ &+ \mathbf{K}_{\mathrm{b}}\mathbf{r}_i^{\alpha_{\mathrm{t}},\alpha_{\mathrm{s}},\alpha_{\mathrm{b}}-1} + \mathbf{E}\mathbf{r}_{i-1}^{\alpha_{\mathrm{t}},\alpha_{\mathrm{s}},\alpha_{\mathrm{b}}}\Big) \end{aligned}$$

where $\widetilde{\mathbf{K}} = \mathbf{K} + 10\mathbf{K}_{\mathrm{t}} + 10\mathbf{K}_{\mathrm{s}} + 10\mathbf{K}_{\mathrm{b}}$ and $\mathbf{r}_0^{0,0,0} = \widetilde{\mathbf{K}}^{-1}\mathbf{b}$.

Let us first consider a PIMTAP model with $(p, q) = (30, 2)$. The corresponding projection subspace $\mathcal{V}$ is given by

$$\mathcal{V} = \mathrm{span}\left\{\mathbf{r}_i^{\alpha} : |\alpha| = 0, 1, 2; i = 0, 1, 2, \ldots, 30\right\}. \tag{37}$$

By (35), the total number of basis vectors is $n(3, 30, 2) = 310$. Due to the deflations among these basis vectors, the actual dimension of $\mathcal{V}$ is 165. The numerical results show that the maximum relative errors at a selected points $(\lambda_{\mathrm{t}}, \lambda_{\mathrm{s}}, \lambda_{\mathrm{b}})$ on the frequency range [0, 100] Hz are $\mathcal{O}(10^{-3})$.

To compare with the method presented in [23], we apply *a priori* physical knowledge that the film coefficient λ_{t} plays a major role. Hence, the projection subspace is chosen to include only those vectors $\mathbf{r}_i^{\alpha}$ corresponding to λ_{t} and s

$$\mathcal{V} = \mathrm{span}\left\{\begin{matrix} \mathbf{r}_0^{0,0,0}, \mathbf{r}_1^{0,0,0}, \mathbf{r}_2^{0,0,0}, \ldots\ldots\ldots, \mathbf{r}_{27}^{0,0,0}, \\ \mathbf{r}_0^{1,0,0}, \mathbf{r}_1^{1,0,0}, \mathbf{r}_2^{1,0,0}, \ldots\ldots\ldots, \mathbf{r}_{27}^{1,0,0}. \end{matrix}\right\}. \tag{38}$$

We observed that the maximum relative errors are $\mathcal{O}(10^{-3})$ on the frequency range [0, 100] Hz. The dimension of PIMTAP model is 49 instead of 56 due to the deflations.

In fact, PIMTAP has the flexibility to match different number of moments corresponding to different parameters. For example, we use the following projection subspace to match only eight moments associated with the geometric parameter λ_{t}

$$\mathcal{V} = \mathrm{span}\left\{\begin{matrix} \mathbf{r}_0^{0,0,0}, \mathbf{r}_1^{0,0,0}, \mathbf{r}_2^{0,0,0}, \ldots\ldots\ldots, \mathbf{r}_{27}^{0,0,0}, \\ \mathbf{r}_0^{1,0,0}, \mathbf{r}_1^{1,0,0}, \ldots, \mathbf{r}_7^{1,0,0}. \end{matrix}\right\}. \tag{39}$$

It is has the same accuracy as reported in [23], which applies *a priori* knowledge of the system to construct a projection subspace through a union of two Krylov subspaces with respect to frequency s and film coefficient λ_{t}. The dimension of the reduced-order model in [23] is 41, higher than the PIMTAP model of order 35.

VII. CONCLUDING REMARKS

The main contributions of this paper are twofold. We give a rigorous definition of the projection subspace for the multiparameter moment-matching property (9). We present a stable and efficient numerical procedure to generate an orthonormal basis of the projection subspace. The new Arnoldi-like procedure exploits the two directional recurrence relationship among the moment generating vectors and is referred to as a TAP. The resulting PIMTAP reduced-order model has the same form of the original system and preserves the passivity. As illustrated by Example C, PIMTAP is flexible in matching selected numbers of moments corresponding to different parameters.

APPENDIX A
PROOF OF THE MOMENT-MATCHING PROPERTY (9)

We first recall the following well-known lemma:

Lemma 7.1:

If the matrix $\mathbf{V}$ is orthogonal and $\mathbf{z} \in \mathrm{span}\{\mathbf{V}\}$, then $\mathbf{V}\mathbf{V}^{\mathrm{T}}\mathbf{z} = \mathbf{z}$.

Proof: Let $\mathbf{P} = \mathbf{V}\mathbf{V}^{\mathrm{T}}$. Then, $\mathbf{P}$ is a projector since $\mathbf{P}^2 = (\mathbf{V}\mathbf{V}^{\mathrm{T}})^2 = \mathbf{V}\mathbf{V}^{\mathrm{T}} = \mathbf{P}$. The range of $\mathbf{P}$ is span$\{\mathbf{V}\}$. Therefore, $\mathbf{P}\mathbf{z} = \mathbf{z}$ for every vector $\mathbf{z}$ in the range of $\mathbf{P}$. ■

Let $\mathbf{V}$ be an orthonormal basis of the projection subspace $\mathcal{V}$ (13). To show the moment-matching property (9), it is sufficient to prove the following identity:

$$\mathbf{V}^{\mathrm{T}}\mathbf{r}_i^j = \widehat{\mathbf{r}}_i^j, \qquad i = 0, 1, \ldots, p \quad j = 0, 1, \ldots, q \tag{40}$$

since by Lemma 7.1 and $\widehat{\mathbf{l}} = \mathbf{V}^{\mathrm{T}}\mathbf{l}$, the identity (40) implies

$$m_i^j = \mathbf{l}^{\mathrm{T}}\mathbf{r}_i^j = \widehat{\mathbf{l}}^{\mathrm{T}}\mathbf{V}\mathbf{V}^{\mathrm{T}}\mathbf{r}_i^j = \widehat{\mathbf{l}}^{\mathrm{T}}\mathbf{V}^{\mathrm{T}}\mathbf{r}_i^j = \widehat{\mathbf{l}}^{\mathrm{T}}\widehat{\mathbf{r}}_i^j = \widehat{m}_i^j.$$

To prove (40), we first use induction on the index i to prove

$$\mathbf{V}^{\mathrm{T}}\mathbf{r}_i^0 = \widehat{\mathbf{r}}_i^0, \qquad i = 0, 1, 2, \ldots, p. \tag{41}$$

For the initial step, since $\mathbf{r}_0^0 \in \text{span}\{\mathbf{V}\}$, by Lemma 7.1, we have

$$\mathbf{G}_0\mathbf{r}_0^0 = \mathbf{G}_0(\mathbf{V}\mathbf{V}^{\mathrm{T}}\mathbf{r}_0^0) = \mathbf{b}. \tag{42}$$

Premultiplying (42) by $\mathbf{V}^{\mathrm{T}}$ and using the definition of $\widehat{\mathbf{G}}_0$ and $\widehat{\mathbf{b}}$ yield the equation (41) for $i = 0$

$$\mathbf{V}^{\mathrm{T}}\mathbf{r}_0^0 = (\mathbf{V}^{\mathrm{T}}\mathbf{G}_0\mathbf{V})^{-1}\mathbf{V}^{\mathrm{T}}\mathbf{b} = \widehat{\mathbf{G}}_0^{-1}\widehat{\mathbf{b}} = \widehat{\mathbf{r}}_0^0.$$

For the inductive step, suppose (41) is true for some $i = k$, i.e., $\mathbf{V}^{\mathrm{T}}\mathbf{r}_k^0 = \widehat{\mathbf{r}}_k^0$, we show that it is also true for $i = k+1$. Since $\mathbf{r}_k^0, \mathbf{r}_{k+1}^0 \in \text{span}\{\mathbf{V}\}$, by Lemma 7.1, we have

$$\mathbf{C}_0\mathbf{r}_k^0 = \mathbf{C}_0(\mathbf{V}\mathbf{V}^{\mathrm{T}}\mathbf{r}_k^0), \quad \mathbf{G}_0\mathbf{r}_{k+1}^0 = \mathbf{G}_0(\mathbf{V}\mathbf{V}^{\mathrm{T}}\mathbf{r}_{k+1}^0).$$

Since $\mathbf{G}_0\mathbf{r}_{k+1}^0 = -\mathbf{C}_0\mathbf{r}_k^0$ by the recurrence relation (6), we have

$$\mathbf{V}^{\mathrm{T}}\mathbf{G}_0\mathbf{V}\mathbf{V}^{\mathrm{T}}\mathbf{r}_{k+1}^0 = -\mathbf{V}^{\mathrm{T}}\mathbf{C}_0\mathbf{V}\mathbf{V}^{\mathrm{T}}\mathbf{r}_k^0. \tag{43}$$

Substituting $\widehat{\mathbf{G}}_0$, $\widehat{\mathbf{C}}_0$, and $\widehat{\mathbf{r}}_k^0$ into (43) and premultiplying $\widehat{\mathbf{G}}_0^{-1}$, we have

$$\mathbf{V}^{\mathrm{T}}\mathbf{r}_{k+1}^0 = -\widehat{\mathbf{G}}_0^{-1}\widehat{\mathbf{C}}_0\widehat{\mathbf{r}}_k^0 = \widehat{\mathbf{r}}_{k+1}^0 \tag{44}$$

where the second identity is due to (8). By induction, the identity (41) holds for $i = 0, 1, \ldots, p$.

Next, we use induction on the index j to complete the proof of the identity (40). Assume that $\mathbf{V}^{\mathrm{T}}\mathbf{r}_i^k = \widehat{\mathbf{r}}_i^k$ holds for $i = 0, 1, \ldots, p$, we show that $\mathbf{V}^{\mathrm{T}}\mathbf{r}_i^{k+1} = \widehat{\mathbf{r}}_i^{k+1}$ for $i = 0, 1, \ldots, p$. Since $\mathbf{r}_{i-1}^k, \mathbf{r}_i^k, \mathbf{r}_{i-1}^{k+1}, \mathbf{r}_i^{k+1} \in \text{span}\{\mathbf{V}\}$, by Lemma 7.1, the recurrence relation (6) implies that

$$\begin{aligned}\mathbf{V}^{\mathrm{T}}\mathbf{G}_0\mathbf{V}\mathbf{V}^{\mathrm{T}}\mathbf{r}_i^{k+1} = &-\mathbf{V}^{\mathrm{T}}\mathbf{C}_0\mathbf{V}\mathbf{V}^{\mathrm{T}}\mathbf{r}_{i-1}^{k+1} - \mathbf{V}^{\mathrm{T}}\mathbf{G}_1\mathbf{V}\mathbf{V}^{\mathrm{T}}\mathbf{r}_i^k \\ &- \mathbf{V}^{\mathrm{T}}\mathbf{C}_1\mathbf{V}\mathbf{V}^{\mathrm{T}}\mathbf{r}_{i-1}^k. \end{aligned}\tag{45}$$

Because of $\mathbf{r}_{-1}^{k+1} = \mathbf{r}_{-1}^k \equiv \mathbf{0}$ and the definitions of $\widehat{\mathbf{G}}_0$ and $\widehat{\mathbf{G}}_1$, the equation (45) for $i = 0$ becomes

$$\mathbf{V}^{\mathrm{T}}\mathbf{r}_0^{k+1} = -\widehat{\mathbf{G}}_0^{-1}\widehat{\mathbf{G}}_1\widehat{\mathbf{r}}_0^k = \widehat{\mathbf{r}}_0^{k+1}.$$

Assuming that $\mathbf{V}^{\mathrm{T}}\mathbf{r}_{i-1}^{k+1} = \widehat{\mathbf{r}}_{i-1}^{k+1}$ and using the definitions of $\widehat{\mathbf{G}}_0$, $\widehat{\mathbf{C}}_0$, $\widehat{\mathbf{G}}_1$, and $\widehat{\mathbf{C}}_1$, we show that $\mathbf{V}^{\mathrm{T}}\mathbf{r}_i^{k+1} = \widehat{\mathbf{r}}_i^{k+1}$ from (45)

$$\begin{aligned}\mathbf{V}^{\mathrm{T}}\mathbf{r}_i^{k+1} &= -\widehat{\mathbf{G}}_0^{-1}\widehat{\mathbf{C}}_0\widehat{\mathbf{r}}_{i-1}^{k+1} - \widehat{\mathbf{G}}_0^{-1}\widehat{\mathbf{G}}_1\widehat{\mathbf{r}}_i^k - \widehat{\mathbf{G}}_0^{-1}\widehat{\mathbf{C}}_1\widehat{\mathbf{r}}_{i-1}^k \\ &= \widehat{\mathbf{r}}_i^{k+1}\end{aligned}$$

where the second equality is due to (8).

By induction on the indices i and j, the identity (40) is true for $i = 0, 1, 2, \ldots, p$, and $j = 0, 1, 2, \ldots, q$. ■

APPENDIX B
TAP

Assume that square matrices $\mathbf{A}_{[j]}$ of order $n_{[j]}$ and vectors $\mathbf{b}_{[j]}$ of length $n_{[j]}$ be a sequence of block lower triangular matrices and vectors with conformal dimensions defined as

$$\mathbf{A}_{[j]} = \begin{bmatrix} \mathbf{A}_{[j-1]} & \mathbf{0} \\ \mathbf{A}_{[j,:]} & \mathbf{A}_j \end{bmatrix} \quad \mathbf{b}_{[j]} = \begin{bmatrix} \mathbf{b}_{[j-1]} \\ \mathbf{b}_j \end{bmatrix} \tag{46}$$

for $j = 2, 3, \ldots$, with the initials $\mathbf{A}_{[1]} = \mathbf{A}_1$ and $\mathbf{b}_{[1]} = \mathbf{b}_1$, where $\mathbf{A}_j$ are n_j by n_j matrices, and $\mathbf{A}_{[j,:]}$ are matrices of conformal dimensions. The space

$$\mathcal{K}_k(\mathbf{A}_{[j]}, \mathbf{b}_{[j]}) = \text{span}\left\{\mathbf{b}_{[j]}, \mathbf{A}_{[j]}\mathbf{b}_{[j]}, \ldots, \mathbf{A}_{[j]}^{k-1}\mathbf{b}_{[j]}\right\}$$

is the kth Krylov subspace induced by $\mathbf{A}_{[j]}$ and $\mathbf{b}_{[j]}$, referred to as the (j,k)th *Krylov subspace* for short.

The standard Arnoldi process [25] computes an orthonormal basis of the Krylov subspace with a fixed index j. Here, we consider the situation where both k and j increase. Specifically, if $\mathbf{Q}_k^{[j-1]}$ be an orthonormal basis of the $(j-1,k)$th Krylov subspace $\mathcal{K}_k(\mathbf{A}_{[j-1]}, \mathbf{b}_{[j-1]})$, then the question is how to stably and efficiently compute an orthonormal basis $\mathbf{Q}_k^{[j]}$ of the (j,k)th Krylov subspace $\mathcal{K}_k(\mathbf{A}_{[j]}, \mathbf{b}_{[j]})$.

Note that $\mathbf{A}_{[j]}$ and $\mathbf{b}_{[j]}$ are the bordered matrix and vector as shown in (46). As the consequence of the observation

$$(\mathbf{A}_{[j]})^i\mathbf{b}_{[j]} = \begin{bmatrix} (\mathbf{A}_{[j-1]})^i\mathbf{b}_{[j-1]} \\ \mathbf{w}_i \end{bmatrix}$$

where $\mathbf{w}_i$ is a vector of the length n_j, we can immediately conclude that the orthonormal bases $\mathbf{Q}_k^{[j-1]}$ and $\mathbf{Q}_k^{[j]}$ satisfy the following relation:

$$\mathbf{Q}_k^{[j]} = \begin{bmatrix} \mathbf{Q}_k^{[j-1]}\mathbf{R} \\ \mathbf{L} \end{bmatrix} \tag{47}$$

where $\mathbf{R}$ is a $k \times k$ nonsingular upper triangular matrix and $\mathbf{L}$ is an $n_j \times k$ matrix. By the relation (47), we can derive a computational procedure to compute $\mathbf{R}$ and $\mathbf{L}$ and obtain $\mathbf{Q}_k^{[j]}$ by updating $\mathbf{Q}_k^{[j-1]}$. To limit the length of this paper, the derivation detail of the computational procedure is presented in [28].

In the following, we present a pseudocode of the procedure. On the input, we have an orthogonal matrix $\mathbf{Q}_{k+1}^{[j-1]}$ and an upper Hessenberg matrix $\widehat{\mathbf{H}}_k^{[j-1]}$ for the order-$(j-1,k)$ Arnoldi decomposition induced by $\mathbf{A}_{[j-1]}$ and $\mathbf{b}_{[j-1]}$

$$\mathbf{A}_{[j-1]}\mathbf{Q}_k^{[j-1]} = \mathbf{Q}_k^{[j-1]}\mathbf{H}_k^{[j-1]} + h_{k+1,k}^{[j-1]}\mathbf{q}_{k+1}^{[j-1]}\mathbf{e}_k^{\mathrm{T}}$$

or a compact form

$$\mathbf{A}_{[j-1]}\mathbf{Q}_k^{[j-1]} = \mathbf{Q}_{k+1}^{[j-1]}\widehat{\mathbf{H}}_k^{[j-1]}$$

where

$$\mathbf{Q}_{k+1}^{[j-1]} = \begin{bmatrix} \mathbf{Q}_k^{[j-1]} & \mathbf{q}_{k+1}^{[j-1]} \end{bmatrix}$$

$$\widehat{\mathbf{H}}_k^{[j-1]} = \begin{bmatrix} \mathbf{H}_k^{[j-1]} \\ h_{k+1,k}^{[j-1]}\mathbf{e}_k^{\mathrm{T}} \end{bmatrix}.$$

On the output, we have the matrix $\mathbf{Q}_{k+1}^{[j]}$ and the upper Hessenberg matrix $\widehat{\mathbf{H}}_k^{[j]}$ for the order-(j,k) Arnoldi decomposition induced by $\mathbf{A}_{[j]}$ and $\mathbf{b}_{[j]}$, and $\mathbf{Q}_{k+1}^{[j]}$ is of the form

$$\mathbf{Q}_{k+1}^{[j]} = \begin{bmatrix} \mathbf{Q}_{k+1}^{[j-1]}\mathbf{R} \\ \mathbf{L} \end{bmatrix}$$

where $\mathbf{R}$ is a $(k+1)\times(k+1)$ nonsingular upper triangular matrix and $\mathbf{L}$ is an $n_j\times(k+1)$ matrix. We will use the MATLAB notation in the pseudocode, namely, $\mathbf{r}_i=\mathbf{R}(1:i,i)$, $\mathbf{l}_i=\mathbf{L}(:,i)$. Note that for the clarity of exposition, the superscript $[j-1]$ of $\mathbf{Q}_{k+1}^{[j-1]}$ and $\widehat{\mathbf{H}}_k^{[j-1]}$ is omitted.

TAP

1) $\tau_j=(1+(\|\mathbf{b}_j\|/\gamma_{j-1})^2)^{1/2}$
2) $\gamma_j=\gamma_{j-1}\,\tau_j$
3) $\mathbf{r}_1=1/\tau_j$; $\mathbf{Q}_1^{[j]}(1:n_{[j-1]})=\mathbf{Q}_1\mathbf{r}_1$
4) $\mathbf{l}_1=(\mathbf{b}_j/\gamma_j)$; $\mathbf{q}_1^{[j]}(n_{[j-1]}+1:n_{[j]})=\mathbf{l}_1$
5) $\widehat{\mathbf{H}}_0^{[j]}=[\,]$
6) for $i=1,2,\ldots,k$
7) $\quad\mathbf{x}_{\rm t}=\widehat{\mathbf{H}}_k(1:i+1,1:i)\,\mathbf{r}_i$
8) $\quad\mathbf{V}_{\rm b}:=\mathbf{A}_{[j,:]}\mathbf{q}_i^{[j]}(1:n_{[j-1]})+\mathbf{A}_j\mathbf{l}_i$
9) $\quad$for $\ell=1,2,\ldots,i$
10) $\quad\quad h_{\ell,i}=\mathbf{r}_\ell^{\rm T}\,\mathbf{x}_{\rm t}(1:\ell)+\mathbf{l}_\ell^{\rm T}\,\mathbf{V}_{\rm b}$
11) $\quad\quad\mathbf{x}_{\rm t}(1:\ell):=\mathbf{x}_{\rm t}(1:\ell)-h_{\ell,i}\,\mathbf{r}_\ell$
12) $\quad\quad\mathbf{v}_{\rm b}:=\mathbf{v}_{\rm b}-h_{\ell,i}\,\mathbf{l}_\ell$
13) $\quad$end for ℓ
14) $\quad h_{i+1,i}=(\|\mathbf{x}_{\rm t}\|^2+\|\mathbf{v}_{\rm b}\|^2)^{1/2}$
15) $\quad$If $h_{i+1,i}=0$, break
16) $\quad\mathbf{r}_{i+1}=\mathbf{x}_{\rm t}/h_{i+1,i}$;
$\quad\mathbf{q}_{i+1}^{[j]}(1:n_{[j-1]})=\mathbf{q}_{i+1}\mathbf{r}_{i+1}$
17) $\quad\mathbf{l}_{i+1}=\mathbf{v}_{\rm b}/h_{i+1,i}$
$\quad\mathbf{q}_{i+1}^{[j]}(n_{[j-1]}+1:n_{[j]})=\mathbf{l}_{i+1}$
18) $\quad\widehat{\mathbf{H}}_i^{[j]}=\begin{bmatrix}\widehat{\mathbf{H}}_{i-1}^{[j]} & \mathbf{h}_i\\ \mathbf{0} & h_{i+1,i}\end{bmatrix}$
19) end for i

Two remarks are in order: 1) The scalar γ_{j-1} in line 1 is a scaling factor such that the vector $\widehat{\mathbf{b}}_{[j]}=[(\mathbf{q}_1^{[j-1]})^{\rm T}(\mathbf{b}_j/\gamma_j)^{\rm T}]^{\rm T}$ is parallel to the vector $\mathbf{b}_{[j]}$, and thus $\mathcal{K}_k(\mathbf{A}_{[j]},\widehat{\mathbf{b}}_{[j]})=\mathcal{K}_k(\mathbf{A}_{[j]},\mathbf{b}_{[j]})$. The norm of the vector $\widehat{\mathbf{b}}_{[j]}$ is computed in line 1. The sequence $\{\gamma_j\}$ is defined by $\gamma_j=\|\widehat{\mathbf{b}}_{[j]}\|\gamma_{j-1}>0$ with the initial $\gamma_1=\|\mathbf{b}_{[1]}\|$ and γ_j is computed in line 2.

2) If the matrix $\mathbf{A}_{[j]}$ and the vector $\mathbf{b}_{[j]}$ are of the type (34), we do not explicitly compute $\mathbf{A}_{[j,:]}$, $\mathbf{A}_j$ and $\mathbf{b}_j$. We can use a recursive algorithm similar to the one presented in [7] for the vector $\mathbf{b}_j$ in lines 1 and 4, and the matrix-vector multiplications associated with $\mathbf{A}_{[j,:]}$ and $\mathbf{A}_j$ in line 8.

ACKNOWLEDGMENT

The authors would like to thank the referees for valuable comments and suggestions to improve the presentation of this paper.

REFERENCES

[1] J. Wang, P. Ghanta, and S. Vrudhula, "Stochastic analysis of interconnect performance in the presence of process variations," in *Proc. IEEE/ACM Int. Conf. Comput.-Aided Des.*, 2004, pp. 880–886.

[2] J. M. Wang, O. A. Hafiz, and J. Li, "A linear fractional transform (LFT) based model for interconnect parametric uncertainty," in *Proc. 41st IEEE/ACM Des. Autom. Conf.*, 2004, pp. 375–380.

[3] P. Gunupudi, R. Khazaka, and M. Nakhla, "Analysis of transmission line circuits using multidimensional model reduction techniques," *IEEE Trans. Adv. Packag.*, vol. 25, no. 2, pp. 174–180, May 2002.

[4] P. K. Gunupudi, R. Khazaka, M. S. Nakhla, T. Smy, and D. Celo, "Passive parameterized time-domain macromodels for high-speed transmission-line networks," *IEEE Trans. Microw. Theory Tech.*, vol. 51, no. 12, pp. 2347–2354, Dec. 2003.

[5] Y. Liu, L. T. Pileggi, and A. J. Strojwas, "Model order-reduction of RC(L) interconnect including variational analysis," in *Proc. 36th IEEE/ACM Des. Autom. Conf.*, 1999, pp. 201–206.

[6] P. Li, F. Liu, X. Li, L. T. Pileggi, and S. R. Nassif, "Modeling interconnect variability using efficient parametric model order reduction," in *Proc. IEEE/ACM Des., Autom. Test Eur.*, 2005, pp. 958–963.

[7] X. Li, P. Li, and L. T. Pileggi, "Parameterized interconnect order reduction with explicit-and-implicit multi-parameter moment matching for inter/intra-die variations," in *Proc. IEEE/ACM Int. Conf. Comput.-Aided Des.*, 2005, pp. 806–812.

[8] J. R. Phillips, "Variational interconnect analysis via PMTBR," in *Proc. IEEE/ACM Int. Conf. Comput.-Aided Des.*, 2004, pp. 872–879.

[9] L. Daniel, O. C. Siong, L. S. Chay, K. H. Lee, and J. White, "A multiparameter moment-matching model-reduction approach for generating geometrically parameterized interconnect performance models," *IEEE Trans. Comput.-Aided Design Integr. Circuits Syst.*, vol. 23, no. 5, pp. 678–693, May 2004.

[10] V. H. O. Farle and R. Dyczij-Edlinger, "An Arnoldi-type algorithm for parametric finite element modelling of microwave components," *PAMM*, vol. 5, no. 1, pp. 655–656, Dec. 2005.

[11] P. I. Ortwin Farle, V. Hill, and R. Dyczij-Edlinger, "Ordnungsreduktion linearer zeitinvarianter finite-element-modelle mit multivariater polynomieller parametrierung," *Automatisierungstechnik*, vol. 54, no. 4, pp. 161–169, 2006.

[12] L. Codecasa, "A novel approach for generating boundary condition independent compact dynamic thermal networks of packages," *IEEE Trans. Compon. Packag. Technol.*, vol. 28, no. 4, pp. 593–604, Dec. 2005.

[13] L. Feng, "Parameter independent model order reduction," *Math. Comput. Simul.*, vol. 68, no. 3, pp. 221–234, May 2005.

[14] L. H. Feng, E. B. Rudnyi, and J. G. Korvink, "Preserving the film coefficient as a parameter in the compact thermal model for fast electrothermal simulation," *IEEE Trans. Comput.-Aided Design Integr. Circuits Syst.*, vol. 24, no. 12, pp. 1838–1847, Dec. 2005.

[15] J. R. Phillips and L. M. Silveira, "Poor man's TBR: A simple model reduction scheme," *IEEE Trans. Comput.-Aided Design Integr. Circuits Syst.*, vol. 24, no. 1, pp. 43–55, Jan. 2005.

[16] P. Ghanta, S. Vrudhula, R. Panda, and J. Wang, "Stochastic power grid analysis considering process variations," in *Proc. IEEE/ACM Des., Autom. Test Eur.*, 2005, pp. 964–969.

[17] S. Grivet-Talocia, S. Acquadro, M. Bandinu, F. G. Canavero, I. Kelander, and M. Rouvala, "A parameterization scheme for lossy transmission line macromodels with application to high speed interconnects in mobile devices," *IEEE Trans. Electromagn. Compat.*, vol. 49, no. 1, pp. 18–24, Feb. 2007.

[18] K. C. Sou, A. Megretski, and L. Daniel, "A quasi-convex optimization approach to parameterized model order reduction," *IEEE Trans. Comput.-Aided Design Integr. Circuits Syst.*, vol. 27, no. 3, pp. 456–469, Mar. 2008.

[19] A. Odabasioglu, M. Celik, and L. T. Pileggi, "PRIMA: Passive reduced-order interconnect macromodeling algorithm," *IEEE Trans. Comput.-Aided Design Integr. Circuits Syst.*, vol. 17, no. 8, pp. 645–654, Aug. 1998.

[20] Z. Feng and P. Li, "Performance-oriented statistical parameter reduction of parameterized systems via reduced rank regression," in *Proc. IEEE/ACM Int. Conf. Comput.-Aided Des.*, 2006, pp. 868–875.

[21] E. Acar, S. Nassif, Y. Liu, and L. T. Pileggi, "Time-domain simulation of variational interconnect models," in *Proc. Int. Symp. Quality Electron. Des.*, Mar. 2002, pp. 419–424.

[22] P. Heydari and M. Pedram, "Model-order reduction using variational balanced truncation with spectral shaping," *IEEE Trans. Circuits Syst. I, Reg. Papers*, vol. 53, no. 4, pp. 879–891, Apr. 2006.

[23] E. B. Rudnyi, L. H. Feng, M. Salleras, S. Marco, and J. G. Korvink, "Error indicator to automatically generate dynamic compact parametric thermal models," in *Proc. Int. Workshop THERMal INvestigations ICs Syst.*, Sep. 2005, pp. 139–145.

[24] R.-C. Li and Z. Bai, "Structure-preserving model reduction using a Krylov subspace projection formulation," *Commun. Math. Sci.*, vol. 3, no. 2, pp. 179–199, 2005.

[25] W. E. Arnoldi, "The principle of minimized iteration in the solution of the matrix eigenvalue problem," *Quart. Appl. Math.*, vol. 9, pp. 17–29, 1951.

[26] A. Stathopoulos and K. Wu, "A block orthogonalization procedure with constant synchronization requirements," *SIAM J. Sci. Comput.*, vol. 23, no. 6, pp. 2165–2182, 2002.
[27] A. Cuyt, "How well can the concept of Padé approximant be generalized to the multivariate case?" *J. Comput. Appl. Math.*, vol. 105, no. 1/2, pp. 25–50, May 1999.
[28] Y.-T. Li, Z. Bai, and Y. Su, "A two-directional Arnoldi process and its application to parametric model order reduction,"*J. Comput. Appl. Math.*. [Online]. Available: http://dx.doi.org/10.1016/j.cam.2008.05.059

Yung-Ta Li received the B.S. degree in mathematics from National Chung Cheng University, Chia-Yi, Taiwan, R.O.C., in 1996, and the M.S. degree in mathematics from the National Tsing Hua University, Hsinchu, Taiwan, in 1998. He is currently working toward the Ph.D. degree in the Department of Mathematics, University of California, Davis.

His research interests include numerical methods for model reduction and large-scale eigenvalue problems.

Zhaojun Bai received the B.S., M.S., and Ph.D. degrees in computational mathematics from Fudan University, Shanghai, China, in 1982, 1985, and 1988, respectively.

He is a Full Professor with the Department of Computer Science and the Department of Mathematics, University of California, Davis. His major interests include numerical linear algebra, parallel scientific computing, and software development. He was involved in the design and implementation of the numerical linear algebra software package LAPACK and is a coauthor of the LAPACK user's guide.

Yangfeng Su received the B.S. and Ph.D. degrees in computational mathematics from Fudan University, Shanghai, China, in 1986 and 1992, respectively.

He is currently a Full Professor and the Associate Dean of the School of Mathematical Sciences, Fudan University. His research interests include model order reduction and computation of large-scale linear and nonlinear eigenvalue problems.

Xuan Zeng (M'97) received the B.Sc. and Ph.D. degrees in electrical engineering from Fudan University, Shanghai, China, in 1991 and 1997, respectively.

She is currently a Full Professor with the Microelectronics Department and serves as the Director of State Key Laboratory of Application Specific Integrated Circuits (ASIC) and Systems, Fudan University. She was a Visiting Professor with the Electrical Engineering Department, Texas A&M University, College Station, and Microelectronics Department, Technische Universiteit Delft, Delft, The Netherlands, in 2002 and 2003, respectively. Her research interests include design for manufacturability, high-speed interconnect analysis and optimization, analog behavioral modeling, circuit simulation, and ASIC design.

Dr. Zeng received the first-class Award of Electronic Information Science and Technology from the Chinese Institute of Electronics in 2005. She received the second-class Award of Science and Technology Advancement and the Cross-Century Outstanding Scholar Award from the Ministry of Education of China in 2006 and 2002, respectively. She received the award of "IT Top 10" in Shanghai in 2003. She served on the Technical Program Committee of the IEEE/Association for Computing Machinery Asia and South Pacific Design Automation Conference in 2000 and 2005.